NeuroImage: Clinical 21 (2019) 101639

Contents lists available at ScienceDirect

NeuroImage: Clinical

journal homepage: www.elsevier.com/locate/ynicl

# Quantification of spinal cord compression using T1 mapping in patients with cervical spinal canal stenosis – Preliminary experience

Ilko L. Maier[a,*,1], Sabine Hofer[b,**,1], Arun A. Joseph[b,c], K. Dietmar Merboldt[b], Eva Eggert[a], Daniel Behme[d], Katharina Schregel[d], Christian von der Brelie[e], Veit Rohde[e], Jan Koch[a], Marios-Nikos Psychogios[d], Jens Frahm[b,c], Jan Liman[a,2], Mathias Bähr[a,2]

[a] Department of Neurology, University Medical Center Göttingen, Germany
[b] Biomedizinische NMR, Max-Planck-Institut für biophysikalische Chemie, Göttingen, Germany
[c] German Center for Cardiovascular Research (DZHK), partner site Göttingen, Germany
[d] Department of Neuroradiology, University Medical Center Göttingen, Germany
[e] Department of Neurosurgery, University Medical Center Göttingen, Germany

ARTICLE INFO

*Keywords:*
Cervical spinal canal stenosis
Spinal cord compression
Cervical spondylotic myelopathy
T1 relaxometry
T1 mapping
MRI

ABSTRACT

*Background:* Degenerative changes of the cervical spinal column are the most common cause of spinal cord lesions in the elderly. Conventional clinical, electrophysiological and radiological diagnostics of spinal cord compression are often inconsistent.

*Materials and methods:* The feasibility and diagnostic potential of a novel T1 mapping method at 0.5 mm resolution and 4 s acquisition time was evaluated in 14 patients with degenerative cervical spinal canal stenosis (SCS) and 6 healthy controls. T1 mapping was performed in axial sections of the stenosis as well as above and below. All subjects received standard T2-weighted MRI of the cervical spine (including SCS-grading 0-III), electrophysiological and clinical examinations.

*Results:* Patients revealed significantly decreased T1 relaxation times of the compressed spinal cord within the SCS (912 ± 53 ms, mean ± standard deviation) in comparison to unaffected segments above (1027 ± 39 ms, $p < .001$) and below (1056 ± 93 ms, $p < .001$). There was no difference in mean T1 in unaffected segments in patients ($p = .712$) or between segments in controls ($p = .443$). Moreover, T1 values were significantly lower in grade II (881 ± 46 ms, $p = .005$) than in grade I SCS (954 ± 29 ms). Patients with central conduction deficit tended to have lower T1 values within the SCS than patients without (909 ± 50 ms vs 968 ± 7 ms, $p = .069$).

*Conclusion:* Rapid high-resolution T1 mapping is a robust MRI method for quantifying spinal cord compression in patients with cervical SCS. It promises additional diagnostic insights and warrants more extended patient studies.

## 1. Introduction

Degenerative changes of the cervical spinal column are a common age-related process, affecting around 30% of the general population in the 4th decade and up to 90% in the 7th decade (Kellgren and Lawrence, 1958; Lawrence, 1969). These degenerative changes often result in cervical spinal canal stenosis (SCS) and spinal cord compression, which is the most common type of spinal cord lesion in patients older than 55 years and the source of acquired spastic paraparesis or afferent ataxia in the middle and later years of life (Small et al., 1999; Montgomery and Brower, 1992).

Diagnosis and time point of surgical treatment, which is key to favorable neurological outcome, have been shown to be difficult to assess due to widely varying signs and symptoms and the lack of pathognomonic clinical findings (McCormick et al., 2003). Moreover, in a significant number of cases, there is a discrepancy between clinical, electrophysiological and radiological findings, further impairing the process of decision making and treatment recommendations (Kalsi-Ryan et al., 2012; Clair and Bell, 2007; Sun et al., 2017a).

While clinical examination is essential for identifying neurological

* Corresponding author at: Department of Neurology, University Medical Center Göttingen, Robert-Koch-Str. 40, 37075 Göttingen, Germany
** Corresponding author at: Biomedizinische NMR, Max-Planck-Institut für biophysikalische Chemie, Am Fassberg 11, 37077 Göttingen, Germany.
*E-mail addresses:* ilko.maier@med.uni-goettingen.de (I.L. Maier), shofer1@gwdg.de (S. Hofer).
[1] These authors contributed equally to this work.
[2] These authors also contributed equally to this work.

https://doi.org/10.1016/j.nicl.2018.101639
Received 2 April 2018; Received in revised form 22 October 2018; Accepted 9 December 2018
Available online 10 December 2018

deficits caused by spinal cord compression, magnetic resonance imaging (MRI) is the method of choice to reveal its site, extent and etiology. Conventional MRI usually includes T1- and T2-weighted imaging on which compression can be measured by comparing the width of the compressed and non-compressed regions of the spinal cord. In addition, T1-hypointensities and T2-hyperintensities help to indicate irreversible tissue destruction such as myelomalacia or gliosis (Takahashi et al., 1987). However, T1 changes so far suffer from operator-dependent inter-rater assessments (Karpova et al., 2010) and T2 alterations only represent late signs of disease progression and have been shown to indicate poorer outcome after surgery (Fernández de Rota et al., 2007). Given the high variability of clinical, electrophysiological and radiological signs, more reliable imaging biomarkers are needed for a precise quantification of this increasingly relevant disease and to develop a prognostic marker for the timing of surgical interventions.

Quantitative mapping of the T1 relaxation process represents an MRI technique for improved evaluations of both neurological and non-neurological diseases. T1 relaxation times have been shown to depend on a variety of white matter microstructural features such as myelin and non-myelin water content, iron concentration, axonal size and axonal density (Koenig et al., 1990; Vymazal et al., 1999; Gelman et al., 2000; Harkins et al., 2016; Hofer et al., 2016) and a recent study demonstrated the feasibility of T1 mapping in the cervical spinal cord of healthy volunteers with high reproducibility (Battiston et al., 2018).

The aim of this study was to investigate the diagnostic value of a rapid high-resolution T1 mapping method based on a single inversion-recovery experiment with radial undersampling and nonlinear inverse reconstruction technique (Wang et al., 2015) in patients with cervical SCS in order to evaluate its potential to differentiate between different stages of spinal cord compression and its correlation to clinical and electrophysiological findings.

## 2. Material and methods

### 2.1. Subjects

In this prospective, single center pilot study, T1 mapping was performed in 14 patients with cervical SCS, which had been diagnosed previously using standard T1- and T2-weighed MRI. Patients were recruited in the Department of Neurology of the University Medical Center Göttingen and T1 mapping was performed at the Max-Planck-Institut für biophysikalische Chemie in Göttingen, Germany.

Clinical symptoms attributable to cervical spinal cord compression were not mandatory for the inclusion in this study. Exclusion criteria were common contraindications for MRI, intolerance of supine posture and inability to give informed consent. T1 mapping was also performed in 6 healthy subjects including the C2 to C7 segments of the cervical spinal column. All patients and controls underwent sagittal and transversal T2-weighted MRI immediately before T1 mapping to determine the axial slice positions for the cervical stenosis region and the unaffected cervical segments above and below.

Standard T1- and T2-weighted images of patients with SCS as well as of healthy controls were reviewed by an experienced neuroradiologist (DB, > 5 years of experience) blinded to the patients'/healthy controls' history. Patients were assigned to four grades of cervical SCS, based on an MRI-based grading system proposed by Kang et al. (Kang et al., 2011) which ranges from grade 0, i.e. no spinal canal stenosis, to grade III, i.e. deformed spinal cord with increased signal intensity near compressed level in T2-weighted images (see Table 1). Representative T2-weighted mid-sagittal images of two patients with a grade I SCS (patient #2 in Table 2) and grade II stenosis (patient #8) are shown in Fig. 1.

The study was approved by the ethics committee of the University Medicine Göttingen (6/6/17) and carried out in accordance with The Code of Ethics of the World Medical Association (Declaration of Helsinki). All patients and healthy controls gave written informed consent.

**Table 1**
Characteristics of patients with cervical spinal canal stenosis and healthy controls.

| | Patients with cervical SCS ($n$ = 14) | Healthy controls ($n$ = 6) | p-Value |
|---|---|---|---|
| Age (mean ± SD) | 66 ± 10 | 34 ± 9 | < 0.001 |
| Sex (male, %) | 12 (85.7) | 5 (83.3) | 1.000 |
| Height (mean cm ± SD) | 174 ± 8 | 180 ± 7 | 0.142 |
| Body weight (mean kg ± SD) | 74 ± 11 | 87 ± 8 | 0.019 |
| Height of SCS (n, %) | | | |
| C2/3 | 0 (0) | 0 (0) | |
| C3/4 | 1 (7.1) | 0 (0) | |
| C4/5 | 2 (14.3) | 0 (0) | |
| C5/6 | 8 (57.1) | 0 (0) | |
| C6/7 | 3 (21.4) | 1 (14.3) | |
| C7/Th1 | 0 (0) | 0 (0) | |
| Grade of SCS (median, IQR) | 2 (1–2) | 0 (0–0.25) | 0.001 |
| Grade 0 (n, %) | 0 (0) | 6 (83.3) | |
| Grade I (n, %) | 6 (42.9) | 1 (16.6) | |
| Grade II (n, %) | 7 (50) | 0 (0) | |
| Grade II and III (n, %) | 1 (7.1) | 0 (0) | |
| History of spine surgery (n, %) | 3 (21.4) | 0 (0) | 0.521 |
| Clinical scores | | | |
| JOA (score, IQR) | 15 (13.75–16.13) | 17 (17–17) | 0.002 |
| Grip and release test (number of grip/releases, IQR) | 21 (16.5–31) | 32 (30.75–36.5) | 0.006 |
| Pain VAS | 1 (0–3.25) | 0 (0–0) | 0.042 |

SCS = spinal canal stenosis; SD = standard deviation; JOA = Japanese Orthopaedic Association score; VAS = visual analogue scale for pain.

### 2.2. Clinical and electrophysiological data

Patients and controls were evaluated using the Japanese Orthopaedic Association (JOA) scale, which ranges from 0 (severe deficits) to 17 points (normal function) (Fukui et al., 1990), the Grip and Release Test (Ono et al., 1987) and a Visual Analogue Scale (VAS) for pain, ranging from zero (no pain) to 10 (maximum of pain). Electrophysiological studies included measurements of the motor-evoked and sensory-evoked potentials to diagnose central conduction deficits. Measurements were conducted in the neurophysiological laboratory of the Department of Neurology of the University Medical Center Göttingen using the Natus Nicolet EDX system and evaluated using Natus Viking software (Natus Neurology Incorporated, Middleton, WI, USA). For motor-evoked potentials, cut-off for the diagnosis was a central motoric conduction time of > 10 ms (M. adductor minimi) or > 15 ms (for *M. tibialis* anterior; cut-off for total conduction time for patients with age < 60 years was 30 ms and 32 ms for patients > 60 years). For sensory-evoked potentials, cut-off for a central conduction deficit was an N20 > 22 ms (median nerve; normal N10) and a P40 > 45 ms (tibial nerve; normal N22). In our neurophysiological laboratory, corrections of conduction times are only applied in patients with heights > 190 cm or < 160 cm, which was neither the case in the patient nor in the control group.

### 2.3. T1 mapping

MRI studies were conducted at 3 T (Magnetom Prisma, Siemens Healthcare Erlangen, Germany) using a 64-channel head coil. Anatomical images were based on a T2-weighted Fast Spin-Echo sequence with in-plane resolution of 0.7 mm and a slice thickness of 3 mm (repetition time TR = 4280 ms, echo time TE = 89 ms, flip angle 120°). In patients, single-slice T1 mapping was performed in three sections, i.e.

**Table 2**
T1 relaxation times in patients with cervical spinal canal stenosis.

| Patient # | Grade of stenosis | T1 relaxation time | | | ΔT1 |
|---|---|---|---|---|---|
| | | Above stenosis | Within stenosis | Below stenosis | |
| 1 | I | 1028 | 966 | 1098 | 97 |
| 2 | I | 1063 | 983 | 1084 | 91 |
| 3 | I | 1083 | 975 | 1003 | 67 |
| 4 | I | 1007 | 923 | 1108 | 135 |
| 5 | I | 1036 | 962 | 1060 | 87 |
| 6 | I | 1000 | 913 | 1075 | 125 |
| 7 | II | 1003 | 911 | 1079 | 131 |
| 8 | II | 974 | 800 | 1115 | 245 |
| 9 | II | 1000 | 888 | 1013 | 118 |
| 10 | II | 1075 | 946 | 1074 | 129 |
| 11 | II | 983 | 902 | 781 | −20 |
| 12 | II | 1015 | 901 | 1012 | 113 |
| 13 | II | 1103 | 837 | 1189 | 309 |
| 14 | II | 1008 | 864 | 1089 | 185 |
| Mean ± SD | | 1027 ± 39 | 912 ± 53 | 1056 ± 93 | 129 ± 78 |

ΔT1 = (T1 above stenosis + T1 below stenosis)/2 − T1 in stenosis.
Mean T1 values in stenosis are significantly different to other regions $p < 0.001$.

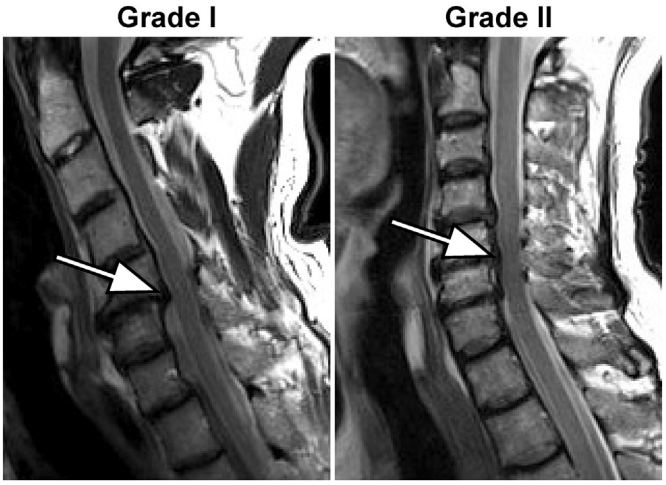


**Fig. 1.** Representative mid-sagittal, T2-weighted MR images of two patients with grade I (patient #2) and grade II SCS (patient #8) without and with spinal cord deformation (arrows), respectively. Both patients present without T2-hyperintensity in the spinal cord.

in the center of the spinal canal stenosis as well as above and below the stenosis with a minimum distance of one segment. In healthy controls, T1 mapping was performed at 6 locations including the C2 to C7 segments of the cervical spinal column. All sections were selected on sagittal T2-weighted images.

T1 mapping of the spinal column was performed at 0.5 mm in-plane resolution and 5 mm slice thickness in multiple axial sections perpendicular to the spinal cord. The used method is based on a single inversion-recovery experiment with a leading slice-selective 180° inversion pulse, a highly undersampled radial gradient-echo readout and a nonlinear inverse image reconstruction technique, for details see (Wang et al., 2015). Briefly, the method employs a low-flip angle gradient-echo sequence (TR = 3.81 ms, TE = 2.60 ms, flip angle 6°) with a small golden-angle radial trajectory (angle = 20.89°) and radiofrequency spoiling by random phase alterations (Roeloffs et al., 2016). In order to optimize computational speed, binning of the data involved 17 spokes per frame and resulted in a temporal resolution of 65 ms for sampling the inversion-recovery process. The acquisition of a total of 62 images then yielded a measuring time of 4 s per T1 map.

Immediately after completion of data acquisition, maps of T1 relaxation times are automatically calculated and displayed on the MRI system. The values are obtained by a pixelwise fitting of the exponential signal model (Deichmann and Haase, 1992) to the set of reconstructed serial images. The parametric results are the equilibrium magnetization $M_0$, the steady-state magnetization $M_{ss}$ and the effective relaxation rate $1/T1^*$ yielding $T1 = T1^* ((M_{ss} - M_0)/M_{ss} - 1)$.

Mean T1 values of the spinal cord were obtained by manually drawing a conservative region-of-interest (ROI) of the myelon using both grayscale T1 maps without artificial color borders and corresponding T2-weighted anatomical images. Color-coded T1 maps are only used for improved visualization. It should be noted that the high spatial resolution of the T1 maps served to minimize partial volume effects with cerebrospinal fluid which has a much longer T1 value and is easily distinguishable from spinal cord and bony structures (low signal). Data analysis and ROI definition were performed using Fiji (*Fiji Is Just ImageJ*), an open source image processing package based on ImageJ (Schindelin et al., 2012) and MATLAB (MathWorks, Natik, MA).

### 2.4. Statistical analysis

Statistical analysis was performed using SPSS 21 (IBM SPSS Statistics, Armonk, NY, USA). Baseline characteristics of all patients and controls are shown as mean ± standard deviation (SD), if normally distributed, and as median with interquartile range (IQR), if not. T1 relaxation times were compared using one-way ANOVA with repeated measurements and post-hoc Bonferroni correction for multiple comparisons at a threshold of $p < .05$. Correlations between clinical or radiological scores and T1 relaxation times were determined by a bivariate Pearson-correlation. *P*-values below 0.05 were considered statistically significant.

## 3. Results

### 3.1. Patient characteristics

The mean age of the 14 patients (Table 1) with degenerative cervical SCS was 66 ± 10 years (34 ± 9 years for the 6 controls, $p < .001$). Twelve (85.7%) patients were male (5 (83.3%) male controls). The maximum extension of the cervical SCS was most frequently found in the C5/C6 segment (8/14 patients) followed by the C6/C7 segment (3/14 patients) and C4/C5 segment (2/14 patients). Most patients had a grade II cervical SCS (8/14 patients) followed by grade I stenosis (6/14 patients). One of these patients had both a grade II stenosis at C5/C6 and a grade III stenosis at C6/C7. In this case (patient #13), the statistical analysis of T1 relaxation times only involved the

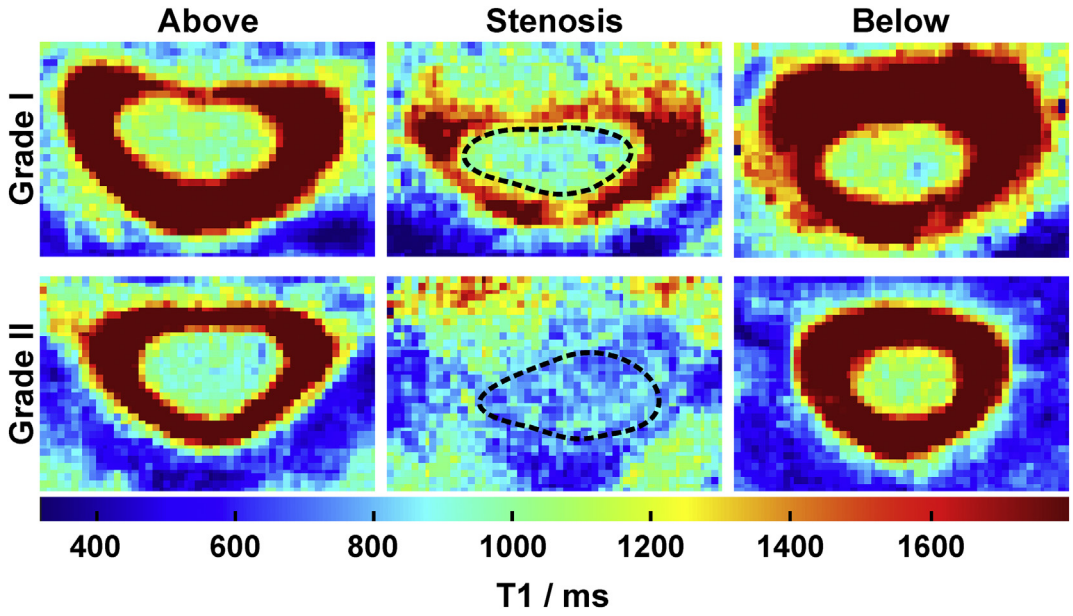


**Fig. 2.** Representative T1 maps of two patients with grade I and grade II SCS (patients #2 and #8 as in Fig. 1). Regions-of-interest were defined on grayscale T1 maps and T2-weighted images. Mean T1 values in SCS regions are lower than in unaffected areas above and below the stenosis.

grade II stenosis, while all four T1 values are shown in Supplementary Fig. 1. One clinically healthy control presented with a low-grade cervical SCS caused by multiple disc bulgings. This patient was excluded from the MRI analysis.

With a median JOA of 15 points (range 13.75–16.13) and a median pain-VAS of 1.0 points (range 0–3.25), patients were clinically only mildly affected by the SCS. Number of grip releases in 10 s was 21 (range 16.5–31) in SCS patients and lower compared to 32 (range 31–38, $p = .003$) in healthy controls.

### 3.2. T1 mapping

As shown in Table 2, T1 relaxation times in the cervical SCS were significantly lower (912 ± 53 ms, mean ± standard deviation) than in non-stenotic segments above (1027 ± 39 ms, $p < .001$) and below (1056 ± 93 ms, $p < .001$). The corresponding mean T1 difference between unaffected segments of the spinal cord and the cervical SCS was 129 ± 78 ms, while there was no difference in mean T1 relaxation times between unaffected segments ($p = .712$). As shown in Figs. 2 and 3, T1 relaxation times in a grade II stenosis were lower (881 ± 46 ms) than values in a grade I stenosis (954 ± 29 ms; $p = .005$).

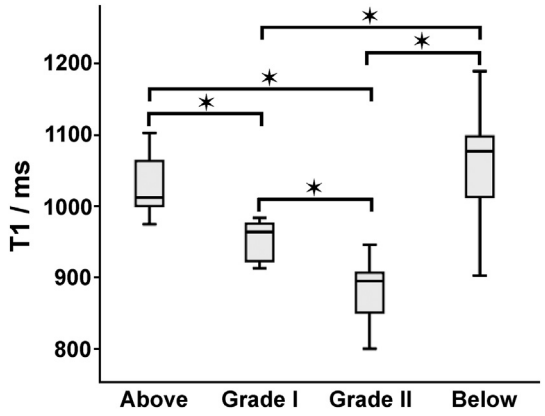


**Fig. 3.** T1 relaxation times (mean ± standard deviation) in patients with grade I and grade II SCS. T1 relaxation times of the compressed spinal cord are significantly lower than above and below the stenosis ($p = .001$). T1 relaxation times are also significantly lower in grade II than in grade I ($p < .005$).

For a single subject, Fig. 4 demonstrates that T1 mapping in healthy controls robustly covered all 6 locations from C2 to C7. The mean T1 relaxation time in healthy controls was 977 ± 45 ms. Individual values revealed no significant variation along the cervical spine ($p = .443$) as shown in Fig. 5. The latter finding is in agreement with a recent T1 study of healthy young controls (Battiston et al., 2018), although the reported T1 values of 1100 to 1150 ms were slightly higher. This may be explained by the use of an EPI-based multi-slice inversion-recovery technique with much lower temporal sampling than used here and a 4-fold lower spatial resolution which is prone to partial volume effects with long T1 values from cerebrospinal fluid.

### 3.3. T1 relaxation times, electrophysiological and clinical findings

From 14 patients with SCS, 11 had a central conduction deficit confirmed by electrophysiological studies (Table 3). These patients tended to have lower T1 relaxation times within the stenosis (909 ± 50 ms vs 968 ± 7 ms, $p = .069$) and a correspondingly higher deviation (ΔT1 value) from unaffected segments of the spinal cord (130 ± 66 ms vs 84 ± 15 ms, $p = .261$). In addition, patients with central conduction deficit showed a strong trend towards having a higher grade of stenosis compared to patients without central conduction deficit (grade II (I-II) vs grade I (I—I), $p = .055$). All healthy controls showed normal electrophysiological data.

There was a negative correlation between the grip and release test and the decrease in T1 relaxation time within the stenosis ($r = -0.546$, $p = .035$), while there was no significant correlation between other scales (JOA and pain-VAS) and T1 relaxation time (data not shown).

## 4. Discussion

The present study for the first time demonstrates the feasibility and diagnostic potential of a rapid high-resolution T1 mapping method to quantitatively assess spinal cord compression in patients with cervical SCS. T1 relaxation times at the site of spinal cord compression not only differed relative to unaffected segments, but also helped to quantify its degree in relation to an established grading system (Kang et al., 2011).

Apart from a proper quantification of spinal cord compression and in view of its potential as a sensitive imaging marker complementary to

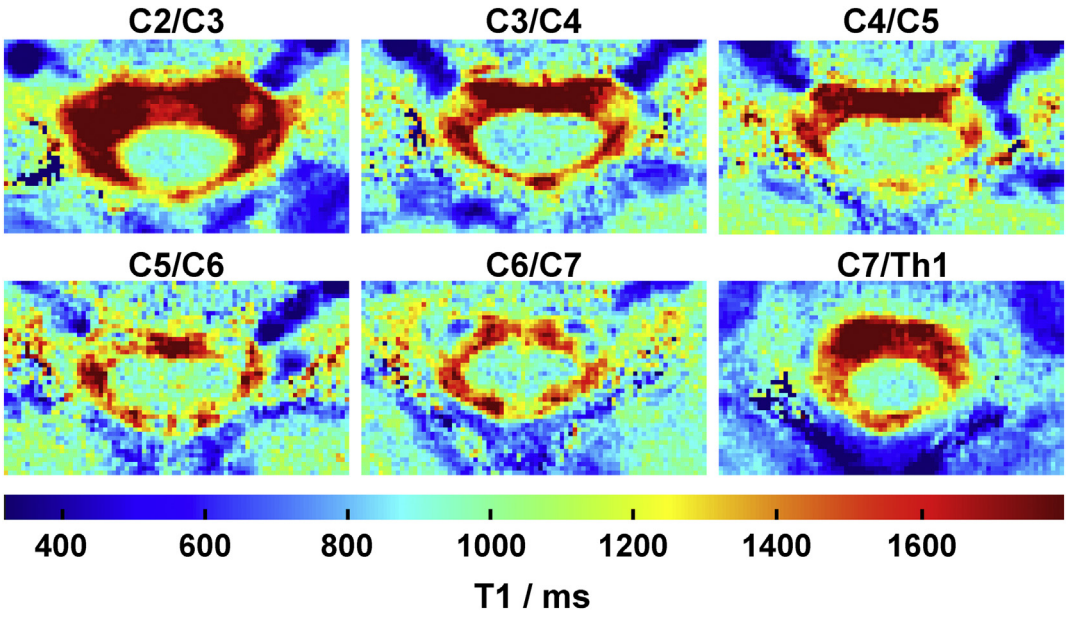


**Fig. 4.** Representative T1 maps of a healthy control in 6 locations along the cervical spinal canal.

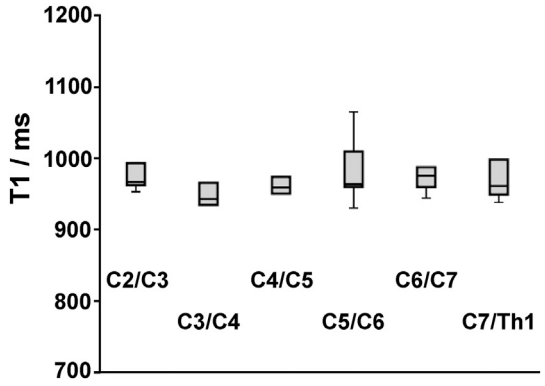


**Fig. 5.** T1 relaxation times (mean ± standard deviation) of healthy controls in positions C2/C3 to C7/Th1 reveal no significant variation along the cervical spinal canal ($p$ = .480).

conventional diagnostics, our novel finding is a T1 decrease in the spinal cord of patients with grade I stenosis. Although these patients without pronounced clinical or electrophysiological abnormalities do not present with a deformation of the spinal cord on T2-weighted MRI, at least not in supine posture, this observation suggests that intermittent compression and deformation of the spinal cord takes place in grade I SCS patients. These dynamic alterations have recently been studied with use of a kinetic MRI technique (Zou et al., 2008; Zeng et al., 2016) and shown to trigger surgical treatment with favorable outcome (Sun et al., 2017b). Together, these findings may explain the frequent discrepancies between conventional MRI, electrophysiology and clinical signs, as also intermittent compression and deformation is likely to cause clinical symptoms and permanent spinal cord dysfunction, while not visible on conventional T2- or T1-weighted MRI. With respect to practicality, however, the speed, robustness and sensitivity of T1 mapping may be superior to kinetic MRI because flexion and extension of the neck is limited in most MRI scanners. Moreover, dynamic studies alone potentially miss other aspects of the disease such as fibrosis or axonal damage. In contrast, the present data indicate that T1 mapping indeed detects changes of the spinal cord, which are due to both intermittent (grade I stenosis) and continuous compression (grade II stenosis) without changing the posture of the patient in the scanner and independent of SCS location.

At this stage it is not entirely clear, which microstructural effects cause the decrease in T1 relaxation time at the site of cervical spinal cord compression. The T1 values of densely packed myelin water in white matter are typically lower than non-myelin cellular water in gray matter (Koenig et al., 1990; Hofer et al., 2016) and degenerative alterations with ischemia and demyelination usually increase the T1 relaxation times of affected tissue. In this respect, Liu et al. could demonstrate a reduced myelin water fraction in patients with pathologic sensory-evoked potentials and cervical spondylotic myelopathy, indicating that a reduction in myelin water is a surrogate for spinal cord compression and dysfunction (Liu et al., 2017). Considering the results of the present study, one may therefore speculate that the main contribution to the T1 decrease is a direct physical consequence of compression compacting the microstructure and squeezing free water molecules with long T1 relaxation times out of the affected spinal cord.

**Table 3**
T1 relaxation times and clinical scores in patients with cervical spinal canal stenosis according to the presence of central conduction deficits.

| | Central conduction deficit ($n$ = 11) | No central conduction deficit ($n$ = 3) | p-value |
|---|---|---|---|
| T1 in stenosis (ms ± SD) | 909 ± 50 | 968 ± 7 | 0.069 |
| ΔT1 (ms ± SD) | 130 ± 66 | 84 ± 15 | 0.261 |
| Grade of stenosis (median, IQR) | II (I-II) | I (I–I) | 0.055 |
| JOA (median score, IQR) | 15 (13–16) | 17 (14–17) | 0.192 |
| Pain VAS (median score, IQR) | 0 (0–3) | 0 (0–4) | 0.214 |
| Grip and release test (median, IQR) | 22 (17–31) | 18 (15–18) | 0.802 |

SD: standard deviation; IQR: Interquartile range; JOA: Japanese Orthopaedic Association scale; VAS: visual analogue scale; ΔT1 = (T1 above stenosis + T1 below stenosis)/2 – T1 in stenosis.

Conversely, the higher T1 relaxation time in the grade III stenosis compared to a grade II stenosis in one patient suggests enhanced contributions from water molecules with longer T1 values that may reflect edematous tissue at the site of maximum compression and structural damage. Nevertheless, further experimental studies are needed to investigate the neuropathological correlates of T1 changes in both acute and chronic spinal cord compression.

In general, also other MRI-detectable metrics such as T2 (or T2*) relaxometry and diffusion-weighted MRI may be able to quantify alterations in cellular density or mobile water content. However, in comparison to T1 mapping as used here, these strategies are much more time-consuming and further involve offline post-processing. Moreover, EPI-based diffusion MRI measurements of the spinal cord often suffer from a pronounced sensitivity to motion and magnetic field inhomogeneity.

This study failed to demonstrate a convincing correlation between T1 relaxation times and clinical signs suggestive for SCS. A likely explanation is the fact that the patients were only mildly affected. The observed T1 alterations therefore do not correspond to advanced or irreversible damages of the spinal cord but refer to intermittent spinal cord deformation (in grade I stenosis) and persistent spinal cord compression yet without irreversible damage (in grade II stenosis). This may, however, represent an interesting surrogate marker to predict future clinical deterioration and therefore may aid decision for or against surgery. This hypothesis needs to be further evaluated in a larger study including follow-up examinations in the future. Another limitation is the low number of patients in this pilot study which leads to a high variability of clinical signs and features. Moreover, the control subjects are not age-matched to the group of patients due to various factors impairing the process of recruiting such a group of entirely healthy subjects (no degenerative changes in MRI, normal electrophysiology and clinical examination plus co-morbidities likely to cause gait disturbances). Further studies should also address age differences concerning T1-relaxation times in elderly patients without SCS, as the present study is unable to demonstrate age dependent changes of T1-relaxation times in unaffected regions of the spinal cord. The question, if age dependent changes exist due to a more densely structured spinal cord in young subjects or an increasing loss of myelinated axons and concomitant enhancement of cellular water with prolonged T1 values with age need to be addressed to provide more evidence for the potential of T1-mapping in the spinal cord as a marker for spinal cord compression and clinical decision making.

## 5. Conclusion

Rapid high-resolution T1 mapping in patients with cervical SCS is time-efficient, robust and accurate. It may significantly enrich the set of diagnostic tools for clinical decision making. Larger studies are needed to correlate T1 relaxation times to clinical signs of the disease and to investigate longitudinal T1 changes associated with conservative or surgical treatment.

## Ethics approval and consent to participate

The study was approved by the ethics committee of the University Medicine Göttingen (6/6/17) and carried out in accordance with The Code of Ethics of the World Medical Association (Declaration of Helsinki). All patients and healthy controls gave written informed consent.

## Consent for publication

All patients and healthy controls included in this study gave written informed consent for the publication of MR images.

## Disclosures

Ilko L. Maier: none.
Sabine Hofer: none.
Arun A. Joseph: none.
K. Dietmar Merboldt: none.
Eva Eggert: none.
Daniel Behme: Speakers' Bureau; Modest; Stryker.
Katharina Schregel: none.
Christian von der Brelie: none.
Veit Rohde: none.
Jan Koch: none.
Marios-Nikos Psychogios: Honoraria; Modest; MNP received speakers' honoraria from Siemens Healthineers.
Jens Frahm: none.
Jan Liman: none.
Mathias Bähr: none.

## Funding

The study was funded by the “Niedersächsische Ministerium für Wissenschaft und Kultur”.

## Acknowledgements

This study was supported by the “Göttinger Kolleg für Translationale Medizin”.

## Author's contribution

Dr. Maier: designed the study and was involved in the acquisition of the data, analyzed raw data, performed statistics, drafted and finalized the manuscript and approved the manuscript before submission.

Dr. Hofer: designed the study and was involved in the acquisition of the data, analyzed raw data, performed statistics, contributed to the manuscript and approved the manuscript before submission.

Dr. Joseph: contributed to the development of the MRI technique, was involved in the acquisition of the data, analyzed raw data, contributed to the manuscript and approved the manuscript before submission.

Dr. Merboldt: was involved in the acquisition of the data, contributed to the manuscript and approved the manuscript before submission.

Ms. Eggert: was involved in the acquisition of the data, contributed to the manuscript and approved the manuscript before submission.

Dr. Behme: was involved in the acquisition of the data, contributed to the manuscript and approved the manuscript before submission.

Dr. Schregel: was involved in the acquisition of the data, contributed to the manuscript and approved the manuscript before submission.

Dr. von der Brelie: contributed to the manuscript and approved the manuscript before submission.

Prof. Dr. Rohde: contributed to the manuscript and approved the manuscript before submission.

Dr. Koch: contributed to the manuscript and approved the manuscript before submission.

Dr. Psychogios: contributed to the manuscript and approved the manuscript before submission.

Prof. Dr. Frahm: designed the study, finalized the manuscript and approved the manuscript before submission.

Dr. Liman: designed the study, contributed to the manuscript and approved the manuscript before submission.

Prof. Dr. Bähr: initiated and designed the study, contributed to the manuscript and approved the manuscript before submission.

## Appendix A. Supplementary data

Supplementary data to this article can be found online at https://doi.org/10.1016/j.nicl.2018.101639.

## References


Battiston, M., Schneider, T., Prados, F., et al., 2018. Fast and reproducible in vivo T1 mapping of the human cervical spinal cord. Magn. Reson. Med. 79, 2142–2148.

Clair, S.S., Bell, G.R., 2007. Natural history of cervical spondylotic myelopathy. Spine Surg. 19, 2–5.

Deichmann, R., Haase, A., 1992. Quantification of T1 values by Snapshot-FLASH NMR imaging. J. Magn. Reson. 96, 608–612.

Fernández De Rota, J.J., Meschian, S., Fernández De Rota, A., Urbano, V., Baron, M., 2007. Cervical spondylotic myelopathy due to chronic compression: the role of signal intensity changes in magnetic resonance images. J. Neurosurg. Spine. 6, 17–22.

Fukui, K., Kataoka, O., Sho, T., Sumi, M., 1990. Pathomechanism, pathogenesis, and results of treatment in cervical spondylotic myelopathy caused by dynamic canal stenosis. Spine Vol. 15, 1148–1152 Phila Pa 1976.

Gelman, N., Ewing, J.R., Gorell, J.M., Spickler, E.M., Solomon, E.G., 2000. Interregional variation of longitudinal relaxation rates in human brain at 3.0 T: relation to estimated iron and water contents. Magn. Reson. Med. 45, 71–79.

Harkins, K.D., Xu, J., Dula, A.N., et al., 2016. The microstructural correlates of T1 in white matter. Magn. Reson. Med. 75, 1341–1345.

Hofer, S., Wang, X., Roeloffs, V., Frahm, J., 2016. Single-shot T1 mapping of the corpus callosum: a rapid characterization of fiber bundle anatomy. Front. Neuroanat. 9, 57.

Kalsi-Ryan, S., Karadimas, S.K., Fehlings, M.G., 2012. Cervical spondylotic myelopathy: the clinical phenomenon and the current pathobiology of an increasingly prevalent and devastating disorder. Neuroscientist 19, 409–421.

Kang, Y., Lee, J.W., Koh, Y.H., et al., 2011. New MRI grading system for the cervical canal stenosis. AJR Am. J. Roentgenol. 197, W134–W140.

Karpova, A., Craciunas, S., Chua, S.Y., Rabin, D., Smith, S., Fehlings, M.G., 2010. Accuracy and reliability of MRI quantitative measurements to assess spinal cord compression in cervical spondylotic myelopathy: a prospective study. Evid. Based Spine Care J. 1, 56–57.

Kellgren, J.H., Lawrence, J.S., 1958. Osteo-arthrosis and disk degeneration in an urban population. Ann. Rheum. Dis. 17, 388–397.

Koenig, S., Brown, R., Spiller, M., Lundbom, N., 1990. Relaxometry of brain: why white matter appears bright in MRI. Magn. Reson. Med. 14, 482–495.

Lawrence, J.S., 1969. Disc degeneration. Its frequency and relationship to symptoms. Ann. Rheum. Dis. 28, 121–138.

Liu, H., MacMillian, E.L., Jutzeler, C.R., et al., 2017. Assessing structure and function of myelin in cervical spondylotic myelopathy: evidence of demyelination. Neurology 89, 602–610.

McCormick, W.E., Steinmetz, M.P., Benzel, E.C., 2003. Cervical spondylotic myelopathy: make a difficult diagnosis, then refer to surgery. Cleve. Clin. J. Med. 70, 899.

Montgomery, D.M., Brower, R.S., 1992. Cervical spondylotic myelopathy: clinical syndrome and natural history. Orthop. Clin. North Am. 23, 487–493.

Ono, K., Ebara, S., Fuji, T., Yonenobu, K., Fujiwara, K., Yamashita, K., 1987. Myelopathy hand. New clinical signs of cervical cord damage. J. Bone Joint Surg. Br. 69, 215–219.

Roeloffs, V.B., Voit, D., Frahm, J., 2016. Spoiling without additional gradients – Radial FLASH MRI with randomized radiofrequency phases. Magn. Reson. Med. 75, 2094–2099.

Schindelin, J., Aganda-Carreras, I., Friese, E., et al., 2012. Fiji: an open-source platform for biological-image analysis. Nat. Methods 28, 676–678.

Small, J.M., Dillin, W.H., Watkins, R.G., 1999. Clinical syndromes in cervical myelopathy. In: Herkowitz, H., Garfin, S.R., Balderson, R.A. (Eds.), The Spine, 4th ed. W.B. Saunders Co, Philadelphia, pp. 465–474.

Sun, Y., Yu, K., Wang, H., Shen, Y., Kong, L., Zhang, J., 2017a. Diagnosis and treatment of hidden lesions in “mild” cervical spondylotic myelopathy patients with apparent symptoms. Medicine (Baltimore) 96, e7623.

Sun, Y., Yu, K., Wang, H., Shen, Y., Kong, L., Zhang, J., 2017b. Diagnosis and treatment of hidden lesions in "mild" cervical spondylotic myelopathy patients with apparent symptoms. Medicine (Baltimore) 96, e7623.

Takahashi, M., Sakamoto, Y., Miyawaki, M., Bussaka, H., 1987. Increased MR signal intensity secondary to chronic cervical cord compression. Neuroradiology 29, 550–556.

Vymazal, J., Righini, A., Brooks, R.A., et al., 1999. T1 and T2 in the brain of healthy subjects, patients with Parkinson disease, and patients with multiple system atrophy: relation to iron Content. Radiology 211, 489–495.

Wang, X., Roeloffs, V., Merboldt, K.D., Voit, D., Schaetz, S., Frahm, J., 2015. Single-shot multi-slice T1 mapping at high spatial resolution – Inversion-recovery FLASH with radial undersampling and iterative reconstruction. Open Med. Imag. J. 9, 1–8.

Zeng, C., Xiong, J., Wang, J.C., et al., 2016. The evaluation and observation of “hidden” hypertrophy of cervical ligamentum flavum, cervical canal, and related factors using kinetic magnetic resonance imaging. Glob. Spine J. 6, 155–163.

Zou, J., Yang, H., Miyazaki, M., et al., 2008. Missed lumbar disc herniations diagnosed with kinetic magnetic resonance imaging. Spine (Phila Pa 1976) 33, E140–E144.